HHS Public Access

Author manuscript

J Immunol. Author manuscript; available in PMC 2016 August 01.

Published in final edited form as:

J Immunol. 2015 August 1; 195(3): 853–864. doi:10.4049/jimmunol.1403114.

Reversing Tolerance in Isotype Switch-Competent Anti-Insulin B Lymphocytes

Jonathan M. Williams[*,†], **Rachel H. Bonami**[†], **Chrys Hulbert**[†], and **James W. Thomas**[*,†,2]

[*]Vanderbilt University, Department of Pathology, Microbiology, and Immunology, Nashville, TN 37232

[†]Department of Medicine, Division of Rheumatology and Immunology, Nashville, TN 37232

Abstract

B lymphocytes that escape central tolerance and mature in the periphery are a liability for developing autoimmunity. IgG insulin autoAbs that predict type 1 diabetes and complicate insulin therapies indicate that mechanisms for tolerance to insulin are flawed. To examine peripheral tolerance in anti-insulin B cells, we generated C57BL/6 mice that harbor anti-insulin VDJ_H-125 site-directed to the native Ig H chain locus (V_H125^{SD}). Class switch-competent anti-insulin B cells fail to produce IgG Abs following T cell-dependent (TD) immunization of V_H125^{SD} mice with heterologous insulin, and they exhibit markedly impaired proliferation to anti-CD40 plus insulin *in vitro*. In contrast, co-stimulation with LPS plus insulin drives robust anti-insulin B cell proliferation. Further, V_H125^{SD} mice produce both IgM and IgG2a anti-insulin Abs following immunization with a conjugate of insulin to type 1 T cell-independent *Brucella abortus* ring test Ag (BRT). Anti-insulin B cells undergo clonal expansion *in vivo* and emerge as IgM^+ and IgM^- $GL7^+$ Fas^+ germinal center (GC) B cells following immunization with insulin-BRT, but not BRT alone. Analysis of Igκ genes in V_H125^{SD} mice immunized with insulin-BRT reveals that anti-insulin Vκ from the pre-immune repertoire are selected into GCs. These data demonstrate that class switch-competent anti-insulin B cells remain functionally silent in TD immune responses, yet these B cells are vulnerable to reversal of anergy following combined BCR/TLR engagement that promotes Ag-specific GC responses and Ab production. Environmental factors that lead to infection and inflammation could play a critical yet under-appreciated role in driving loss of tolerance and promoting autoimmune disease.

Introduction

Tolerance for B lymphocytes in the developing repertoire is maintained first by receptor editing and clonal deletion in the bone marrow (1–3). Not all self-reactive B cells are removed by central tolerance, however, as BCRs with monovalent or weak interactions with autoAgs may avoid elimination or revision (4, 5). Autoreactive B cells that escape central tolerance and mature in the periphery are a liability, and additional mechanisms of tolerance are necessary to guard against autoimmunity (6–9). B cells that continuously encounter self-

[2]Address correspondence and reprint requests to Dr. James W. Thomas, Vanderbilt University Medical School, 1161 21st Avenue South, Medical Center North T-3113, Nashville, TN, 37232. james.w.thomas@vanderbilt.edu. Fax number: 615-322-6248.

Ags may be rendered anergic or functionally silent to immune stimuli in the periphery. Tolerant B cells exhibit decreased surface IgM expression, impaired Ca^{2+} mobilization, restricted competition for available survival factors and follicular niches, and impaired responses to both T cell help and B cell mitogens (7, 10). Such anergic B cells are recognized in both normal and autoimmune repertoires (11–13).

The importance of BCR signaling for maintaining peripheral tolerance is emphasized by the reversal of anergy upon removal of chronic cognate Ag (10, 11). Alterations in BCR signaling pathways and mediators such as phosphoinositide 3-kinase, protein kinase C theta, and the negative regulator protein tyrosine phosphatase non-receptor type 22 have been shown to impact both the induction and maintenance of tolerance (14–16). Innate signaling via toll-like receptors (TLR) and MyD88 reverses anergy in some autoreactive B cells, suggesting that environmental factors that lead to infection and inflammation may also alter tolerance (17, 18). B cells deficient in MyD88 demonstrate impaired IgM responses to bacterial Ags, indicating that innate signaling through TLR pathways is critical for early T cell-independent (TI) immune defense (19). TLR-4 stimulation by LPS unlocks alternate signaling pathways to ERK phosphorylation and NF-κB activation independent of conventional BCR-dependent signaling mediators (20) that may be impaired for anergic B cells. Adaptive interactions with T cells may also drive loss of B cell tolerance and promote somatic hypermutation and Ig class switch recombination (CSR) in germinal center (GC) reactions associated with ongoing autoimmune disorders (21, 22). The fact most pathogenic autoAbs are of the IgG isotype further implicates T cells as potential vectors for driving loss of B cell tolerance. Thus, the overall effectiveness of immune tolerance for B lymphocytes depends on the nature of BCR interaction with autoAgs, potential encounter with innate signals in the environment, and availability of epitopes that promote cognate T-B interactions.

Insulin is a protein hormone whose small size and low circulating concentration was previously thought to limit BCR interactions necessary for tolerance (23, 24). Studies using a conventional IgM-restricted anti-insulin BCR transgene revealed that anti-insulin B cells enter the mature repertoire but are anergic and fail to produce anti-insulin Abs following T cell-dependent (TD) immunization (25). Such functionally silenced B cells residing in the periphery retain cellular functions such as Ag presentation that enable them to promote autoimmunity in NOD mice (22, 26). Insulin autoAbs associated with autoimmune disorders like type 1 diabetes, as well as Abs that arise in response to insulin therapy and complicate disease management, are predominantly of the IgG isotype (27–32). How the ability to undergo CSR contributes to the maintenance or loss of tolerance for anti-insulin B cells is not known. To assess peripheral tolerance in anti-insulin B cells competent to undergo somatic hypermutation and CSR, we generated C57BL/6 (B6) mice that harbor an anti-insulin H chain site-directed to its native locus (V_H125^{SD}). V_H125^{SD} pairs with endogenous L chains to generate a polyclonal B cell repertoire, where physiologically relevant CSR-competent anti-insulin B cells successfully compete and make up a small fraction of the repertoire. V_H125^{SD} B6 mice crossed with anti-insulin Vκ125Tg mice generates a monoclonal B cell repertoire in which > 98% of the B cells bind insulin (V_H125^{SD}/Vκ125Tg), a model utilized for *in vitro* experiments. These two models are used to assess

the fate and function of anti-insulin B cells that are competent to undergo isotype switch in either a monoclonal or polyclonal repertoire.

In this report, we examine how peripheral tolerance is governed for autoreactive B lymphocytes that bind the relevant autoAg, insulin. CSR-competent anti-insulin B cells enter mature compartments but are anergic, demonstrated by impaired proliferation to stimulation by a panel of B cell mitogens *in vitro* and total lack of IgG anti-insulin Ab production following TD immunization of V_H125^{SD} B6 mice. Reversal of anti-insulin B cell anergy is demonstrated by proliferation to insulin plus LPS *in vitro* and IgG2a Ab production following immunization of V_H125^{SD} B6 mice with insulin conjugated to a type 1 TI Ag (24, 33). This combined BCR/TLR co-stimulation effect *in vivo* is accompanied by entry of insulin-binding B cells into GCs, where anti-insulin L chains are not discarded but rather selected from the pre-immune repertoire. These studies reveal a new pathway to drive loss of tolerance for CSR-competent anti-insulin B cells.

Materials and Methods

Targeting vector and generation of V_H125^{SD} mice

$pIV_HL2neoR$ is a vector designed for targeted insertion of a rearranged V_H gene replacing J_H loci, and was a kind gift from Dr. Klaus Rajewsky (34). We first modified $pIV_HL2neoR$ by cloning in two regions of short arm homology (SAH) at *Cla1* and *Not1* sites. This was necessary after initial efforts of homologous recombination were poor. Anti-insulin VDJ_H-125 from our original H chain plus L chain 125Tg mice (25) was sub-cloned into the pGEM-5Z vector and then cloned into modified $pIV_HL2neoR$-SAH at *Sal1* and *Cla1* sites to generate our targeting vector, pIV_H-SAH-125-VDJ_H. All sequences were verified throughout the cloning process. pIV_H-SAH-125-VDJ_H was linearized through digestion with *Not1* and electroporated into 129/Ola ES cells. The electroporated cells were selected for neomycin resistance. ES clone DNA was digested with *Hin*dIII, and Southern blot hybridization using a cDNA probe against an *Xba1* enhancer located upstream of V_H125^{SD} detected the proper 6.1kb fragment size of the construct in the targeted locus. Clones were confirmed by PCR using H chain primers FWD 5'-CAG ATC CAG TTG GTG CAG TC-3' and REV 5'-CCA GAC ATC GAA GTA CCC CT-3'. Positive ES clones were injected into blastocysts and transplanted into pseudopregnant female mice. Tail DNA from founder chimeric pups and their progeny were screened for V_H125^{SD}. Southern blot was used to confirm the presence of the targeted allele.

Mice

V_H125^{SD} mice were backcrossed onto the C57BL/6 (B6) background. B6 mice and MD4 anti-HEL mice (B6-Tg [IghelMD4]4Ccg/J) were purchased from Jackson Laboratory, Bar Harbor, ME. EIIA-Cre B6 mice, kindly provided by Dr. Richard Breyer, Vanderbilt University, were intercrossed with V_H125^{SD} mice to permanently remove the neomycin resistance cassette. Transgene transmission was monitored in subsequent generations of site-directed V_H125^{SD} B6 mice using PCR, and flow cytometry confirmed the presence of > 95% transgenic IgM^{a+} B cells. Male and female mice aged 7–14 wks were used in these studies and backcrossed > 10 times to B6. All animals were housed in specific pathogen free

conditions, and all studies were approved by the AAALAC certified Vanderbilt Institute of Animal Care and Use Committee.

Antibodies and flow cytometry

Abs reactive to murine B220 (RA3–6B2), IgM^a (DS-1), IgM^b (AF6–78), CD21 (7G6), CD23 (B3B4), IgD (11–26), GL7, or Fas/CD95 (Jo2) (BD Pharmingen), or IgM (μ-chain specific, Invitrogen) were used, along with biotinylated human insulin (35) or biotinylated anti-insulin mAb 123 (36) with streptavidin-conjugated fluorochrome to detect insulin-binding B cells, and 7-aminoactinomycin D for cell viability. Flow cytometry acquisition was performed after cell suspension in FACS buffer (1X PBS, 10% FBS, 1% sodium azide, 1% EDTA) using an LSR II (BD Biosciences), and sorting experiments were performed using a FACSAria I or II cell sorter in the Vanderbilt University Shared Resource Facility. Analysis was performed using FlowJo software (Treestar).

Proliferation assays

B cells were purified from whole spleens using negative selection with anti-CD43 magnetic beads (MACS, Miltenyi Biotec). Average B cell purity across all experiments performed: V_H125^{SD}/Vκ125Tg – 91.4%, n = 9; MD4 anti-HEL – 91%, n = 8; Wild-type – 92.5%, n = 3. Cells were plated at 2×10^5 per well in complete RPMI (10% FBS, 1% HEPES, 1% L-Glutamine, 1% gentamycin), and cultured for 72h in a 37°C 5% CO_2 incubator. Cells were pulsed with tritiated thymidine deoxyribose ($[^3H]$-TdR) on d2 and harvested using a semi-automated cell harvester (Skatron) on d3. $[^3H]$-TdR incorporation was measured by scintillation counting, and results are expressed as the mean cpm ± SD for the indicated number of mice in each experimental group. For *in vivo* proliferation experiments, mice were injected i.p. with BrdU per the manufacturer's instructions (BD Pharmingen) 48h and 24h before sacrifice, in both unimmunized and insulin-BRT immunized mice. FITC-conjugated anti-BrdU (BD Pharmingen) was used to detect intracellular incorporation of BrdU.

Immunization and ELISA

For TD assays, pre-immune sera were collected, and mice were immunized with 40–50 μg bovine insulin in 1X PBS emulsified in either CFA s.c. at the base of the tail or in IFA i.p., and sera were collected 2–3 wks later. For TI assays, mice were immunized i.p. with human insulin-conjugated *Brucella abortus* ring test Ag (insulin-BRT) (24), with BRT alone, or with physically mixed BRT and insulin, and sera were collected at 5–7 d following immunization. Anti-insulin Abs were measured by ELISA as follows: briefly, 96-well flat-bottom NUNC plates were coated with human insulin in borate buffered saline overnight at 37°C. Plates were extensively washed with 1X PBS-Tween (0.05%). Diluted sera (1:100) were added to the coated plates with or without 100X soluble human insulin to measure specific, inhibitable anti-insulin Abs. IgM and IgG anti-insulin Abs were detected using the following allotype-specific secondary Abs: IgM^a-biotin (DS-1), $IgG1^a$-biotin (10.9), or $IgG2a^a$-biotin (8.3) for transgenic anti-insulin B cells, or IgM^b-biotin (AF6–78), $IgG1^b$-biotin (B68-2), or $IgG2c^b$-biotin (5.7) (BD Pharmingen) for non-transgenic or WT B cells. Avidin-alkaline phosphatase (AP) (Sigma), or goat anti-mouse IgM-AP or IgG-AP Abs

(Southern Biotech) were added. After washing, p-Nitrophenyl Phosphate substrate (Sigma) was added to the plate and immediately read on a Microplate Autoreader (Bio-Tek Instruments) at O.D. 405 nm. Inhibitable (insulin-specific) binding was determined by the difference in binding in the presence or absence of excess competitive insulin.

Immunohistochemistry

Spleens were removed from unimmunized or insulin-BRT immunized V_H125^{SD} B6 mice and soaked in 30% sucrose (w/v) overnight at 4°C and snap frozen in OCT medium on dry ice. 8 μM sections were obtained from the Vanderbilt Translational Pathology Shared Resource. Sections were fixed with 4% paraformaldehyde in 0.1M PBS and stained with the following Ab cocktails: IgM Alexa Flour 488 (Life Technologies), IgD^a-biotin (AMS 9.1, BD Pharmingen) plus streptavidin Alexa Flour 350 (Life Technologies), and CD3 PE (17A2, BD Pharmingen) to define follicular architecture, or GL7 FITC, IgD^a-biotin plus streptavidin Texas Red (Molecular Probes), and DAPI (Molecular Probes) to detect GCs. Images were obtained using an Olympus BX60 fluorescent microscope with MagnaFire software. Adobe Photoshop was used to adjust brightness and contrast, and to overlay images.

Pancreata were dissected from unimmunized or insulin-BRT immunized V_H125^{SD} B6 mice, or from 12–16 wk old female NOD mice (as a positive control for insulitis assessment) and placed into neutral buffered formalin. After 4–6 h, tissues were transferred to 70% ethanol and incubated overnight. Tissues were subsequently paraffin embedded, 5μm sections were cut, and slides were stained with H&E by the Vanderbilt Translational Pathology Shared Resource. Slides were blind scored for insulitis by light microscopy using the following scale: 0 = no insulitis; 1 = peri-insulitis, < 25% islet infiltration; 2 = 25–50% islet infiltration; 3 = 50–75% islet infiltration; 4 = > 75% islet infiltration. Half of the pancreas was fixed with paraformaldehyde in 0.1M PBS and soaked in 30% sucrose overnight at 4°C, and then snap frozen in OCT medium on dry ice. 8 μM sections were stained for immunofluorescence with DAPI and biotinylated anti-$IgG2a^a$ plus FITC-conjugated streptavidin.

Light chain cloning and sequencing

Spleens were harvested from unimmunized V_H125^{SD} B6 mice, or from mice 4 d following insulin-BRT immunization. Human insulin-binding B cells ($B220^+$ live lymphocytes) were identified by FACS and further gated as IgM^+ non-GC ($GL7^-$ Fas^-), IgM^+ GC ($GL7^+$ Fas^+), or IgM^- GC populations. Cells were sorted directly into RNAqueous lysis buffer, and RNA was isolated using the RNAqueous-Micro Total RNA Isolation Kit per the manufacturer's instructions (Life Technologies). Independent clones were derived from separate tubes of lysate. RNA was reverse transcribed into cDNA using Superscript II RT (Invitrogen) and oligo-dT primer (GE Healthcare) in a standard protocol. Resulting cDNA was used as PCR template to amplify Igκ genes using a murine Vκ primer, 5′−ATT GTK MTS ACM CAR TCT CCA-3′, and murine Cκ primer, 5′−GGA TAC AGT TGG TGC AGC ATC-3′, where K = G or T, M = A or C, S = C or G, and R = A or G with a 44°C annealing temperature. Appropriately sized PCR products were gel purified using the MinElute Gel Extraction Kit (Qiagen) and Igκ were cloned as described previously (37, 38). Vκ and Jκ gene segment

identities were assigned using Ig BLAST (http://www.ncbi.nlm.nih.gov/igblast/) with CDR boundaries defined by the KABAT V domain delineation system. Nucleotide mutation analyses were also performed using the Ig BLAST tool.

Results

A site-directed BCR transgenic mouse model generates class switch-competent anti-insulin B lymphocytes

Previous μ-only BCR transgenic mouse models do not address how native cellular functions like CSR impact the state of immune tolerance for anti-insulin B cells. To examine peripheral tolerance for anti-insulin B cells competent to undergo isotype switch, B6 mice that harbor anti-insulin VDJ_H-125 site-directed to the Ig H chain locus were developed as described in Methods. Fig. 1A summarizes the strategy for generating the targeting construct used to develop site-directed V_H125^{SD} B6 mice. Southern blot, PCR, and flow cytometry confirmed successful Ig H chain locus targeting, as $B220^+$ splenic B cells from V_H125^{SD} B6 mice co-express IgM^a and IgD^a while those from conventional μ-only V_H125Tg B6 mice express only IgM^a as expected (Fig. 1B).

Flow cytometry with biotinylated insulin was used to investigate the contribution of different anti-insulin transgenes to insulin-binding B cells (Fig. 1C). Left, mice that possess only an anti-insulin L chain (Vκ125Tg) show low numbers of insulin-binding B cells in the spleen (0.12 ± 0.01%, n = 3), but these weakly binding cells are not specific, as they are not inhibited with excess competitive insulin (not shown). Center, V_H125^{SD} B6 mice have B cells in which the targeted transgene pairs with endogenous L chains to generate a small population of insulin-binding B cells (0.46 ± 0.05%, n = 9) (Fig. 1C). Right, intercrosses that pair V_H125^{SD} with Vκ125Tg confers insulin-binding specificity to > 98% of the B cells. Unlike other site-directed mouse models, such as the SW_{HEL} model (39), V_H gene revision or editing is not prevalent for IgM^+ B cells in V_H125^{SD}, as > 95% are [a] allotype and retain their insulin-binding potential. These data demonstrate a novel site-directed BCR transgenic model can be used to assess the fate and function of CSR-competent anti-insulin B lymphocytes within a monoclonal or polyclonal repertoire.

Anergy in anti-insulin B cells is reversed by TLR-4 but not CD40 co-stimulation in vitro

To determine whether CSR-competent anti-insulin B cells are anergic, B cells were purified from V_H125^{SD}/Vκ125Tg or wild-type (WT) B6 mice using MACS, and tritiated thymidine incorporation was used to assess B cell proliferation *in vitro* to anti-IgM, anti-CD40, or LPS stimulation (Fig. 2). Anti-insulin B cells exhibit impaired proliferative responses to stimulation through BCR, CD40, and TLR-4, compared to B cells from WT B6 mice (Fig. 2A). Thus, anergy is maintained for CSR-competent IgM^{a+} IgD^{a+} anti-insulin B cells *in vitro*, similar to that reported for anti-insulin B cells in conventional μ-only 125Tg mice (H + L chain) (26).

Different co-stimulation pathways were assessed for their impact on proliferation in the context of BCR encounter with autoAg. B cells were purified from V_H125^{SD}/Vκ125Tg B6 mice or naïve anti-HEL MD4-Tg mice (10) and stimulated with anti-CD40 (Fig. 2B) or LPS

(Fig. 2D) in the presence or absence of cognate Ag. Using B cells specific for hen egg lysozyme (HEL) as naïve control, stimulation with HEL plus anti-CD40 at low concentration (0.1 μg/mL) synergized to significantly augment proliferation (30× increase, Fig. 2C). In contrast, stimulation of anti-insulin B cells with insulin plus anti-CD40 did not enhance their proliferation, but instead blunted the response (0.52×, Fig. 2C). Synergy is defined here as the mathematical value representing the effect of B cell co-stimulation relative to the effect of the sum of each individual stimulus. Failure to demonstrate synergy between insulin and anti-CD40 was consistent across a wide range of Ag and Ab concentrations (data not shown). These data suggest anergy is maintained for CSR-competent anti-insulin B cells co-stimulated with cognate Ag and anti-CD40, which mimics T cell help.

Using naïve anti-HEL B cells as control, co-stimulation with HEL and LPS at low concentration (0.1 μg/mL) only marginally boosted proliferation, with no evidence of synergy (1.2×, Fig. 2E). In striking contrast, co-stimulation of anti-insulin B cells with insulin and LPS synergized to enhance B cell proliferation (10×, Fig. 2E). These data demonstrate that *in vitro* responses of anti-insulin B cells are altered by prior exposure of the monoclonal repertoire to Ag *in vivo*. Anti-insulin B cells are anergic, as they fail to proliferate to anti-CD40 with or without Ag. However, this anergy is readily reversed by simultaneous engagement of BCR and TLR-4 *in vitro*.

Anti-insulin B cells from V_H125^{SD} B6 mice undergo peripheral maturation

We sought to understand how the features of tolerance observed in a nearly monoclonal population of anti-insulin B cells apply to a polyclonal repertoire that contains relatively few anti-insulin B cells (V_H125^{SD}). Factors that govern anergy for autoreactive B lymphocytes in a polyclonal repertoire include competition for survival and entry into mature compartmental niches (6, 26, 40, 41). To assess whether CSR-competent anti-insulin B cells in the polyclonal repertoire of V_H125^{SD} B6 mice enter mature subsets, flow cytometry was used to identify B cells ($B220^+$ IgM^{a+} live lymphocytes) that distributed into transitional 1 (T1, $CD21^-$ $CD23^-$), follicular (FO, $CD21^{int}$ $CD23^{high}$), and marginal zone (MZ, $CD21^{high}$ $CD23^{low}$) compartments of the spleen (Fig. 3). In contrast to WT B6 mice, a small population of anti-insulin B cells is observed in V_H125^{SD} B6 mice (0.42 ± 0.05%, n = 9), and their specificity is confirmed by inhibition with unlabeled competitive insulin (Fig. 3A, left panels). Rare insulin-binding B cells in WT B6 mice (0.03 ± 0.01%, n = 3) are not inhibited by excess insulin (Fig. 3A, right panels). The ability of B cells to enter T1, FO, and MZ subsets was compared for non-insulin binding (ins^-) or insulin-binding B cells (ins^+) in V_H125^{SD} B6 mice, or for WT B cells (Fig. 3B). As represented in Fig. 3C, ins^+ B cells predominantly populate the FO subset in V_H125^{SD} B6 mice, whereas fewer ins^+ B cells are found in other subsets (8.1 ± 3.2% T1, 78.9 ± 5.5% FO, 2.7 ± 1.9% MZ, n = 7). The reduced representation of ins^+ B cells in the MZ contrasts ins^- B cells (12.25 ± 2.6% T1, 57.7 ± 3.5% FO, 16.5 ± 1.7% MZ) in V_H125^{SD} B6 mice and normal B cells (8.4 ± 1.7% T1, 78.3 ± 3.7% FO, 6.0 ± 0.9% MZ, n = 6) in WT B6 mice. These data suggest that anti-insulin B cells in the peripheral repertoire of V_H125^{SD} B6 mice are principally mature follicular B cells.

To determine whether anti-insulin B cells are clonally ignorant or if their BCRs have encountered endogenous rodent insulin *in vivo*, a second anti-insulin monoclonal Ab (mAb123) was used. MAb123 recognizes a different insulin epitope and binds insulin-occupied BCRs (25, 35). Flow cytometry staining with mAb123 confirms that BCRs are occupied by endogenous insulin in V_H125^{SD} B6 mice (0.4 ± 0.1%, Fig. 3D). These data demonstrate that CSR-competent anti-insulin B cells in V_H125^{SD} B6 mice successfully compete in a polyclonal repertoire and populate follicular compartments despite encounter with physiologic autoAg during development and early peripheral maturation.

IgM and IgG anti-insulin antibodies are produced in V_H125^{SD} B6 mice following TI but not TD immunization

Prior studies in mice harboring IgM^a-restricted anti-insulin B cells demonstrated failure to respond to TD immunization (25). To dissect the functional status of CSR-competent IgM^{a+} IgD^{a+} anti-insulin B cells in V_H125^{SD} B6 mice, Ab responses were assessed following two different immunization strategies, and IgM and IgG anti-insulin Abs in sera were measured by ELISA (Fig. 4). For TD responses, mice were immunized with bovine insulin emulsified in CFA (insulin/CFA). Bovine insulin was chosen for TD immunization because the MHC-II of B6 mice ($I\text{-}A^b$) is genetically a strong responder to bovine but not to other insulins, notably human (24). Conventional WT B6 mice generated a strong $IgG1^b$ anti-insulin response following insulin/CFA immunization, whereas CSR-competent anti-insulin B cells in V_H125^{SD} B6 mice failed to produce $IgG1^a$ anti-insulin Abs (Fig. 4A). To ensure the absence of response to insulin/CFA immunization in these mice is not attributed to lack of bovine insulin processing by anti-insulin BCRs, we used competitive inhibition in flow cytometry to confirm that bovine insulin at concentrations well below that used in immunization fully competes with human insulin for binding to anti-insulin B cells in V_H125^{SD} B6 mice (Supplemental Figure). IgG1 was the predominant isotype observed following insulin/CFA immunization, a finding that agrees with previous work that examined the Ig response to insulin in B6 mice (24). To test whether TLR signaling provided by *Mycobacteria* in CFA is necessary, mice were also immunized with bovine insulin emulsified in IFA (insulin/IFA). While the $IgG1^a$ anti-insulin response remained absent in V_H125^{SD} B6 mice, WT B6 mice generated $IgG1^b$ anti-insulin Abs following insulin/IFA immunization (data not shown). This agrees with prior studies that demonstrated B cells deficient in both MyD88 and TRIF were able to mount Ab responses to multiple Ags administered in a variety of adjuvants, including CFA and IFA (42). These data validate that tolerance for anti-insulin B cells is maintained for TD immune responses to heterologous insulin, in either the presence or absence of mycobacterial adjuvant.

To assess anti-insulin B cell competence to produce Abs in the absence of cognate T cell help, V_H125^{SD} B6 mice were immunized with human insulin conjugated to *Brucella abortus* ring test Ag (insulin-BRT), or BRT alone (24). Human insulin is used in BRT conjugates to avoid introduction of T cell epitopes. Prior studies showed that insulin-BRT behaves as a typical type 1 TI Ag, including response kinetics, expected Ab isotypes, and responses observed in both athymic and X-linked immunodeficient mice (33, 43). Following immunization with insulin-BRT, B cells from WT B6 mice and CSR-competent anti-insulin B cells from V_H125^{SD} B6 mice produced IgM^b and $IgG2c^b$ or IgM^a and $IgG2a^a$ anti-insulin

Abs, respectively (Fig. 4B). Immunization with BRT alone, however, failed to induce any detectable IgG anti-insulin Abs in either V_H125^{SD} or WT B6 mice (Fig. 4B). Similarly, immunization with physically mixed BRT and insulin failed to induce any response (data not shown). Insulin-BRT immunization did not elicit IgG1 Abs, consistent with the expected isotypes associated with BRT conjugates (33, 43). These data suggest that the insulin-BRT conjugate promotes loss of tolerance for CSR-competent anti-insulin B cells *in vivo* through a combination of BCR and TLR signaling that drives production of IgM and IgG anti-insulin Abs.

To determine the pathological consequences of the breach in tolerance observed in V_H125^{SD} B6 mice following insulin-BRT immunization, pancreata were examined for insulitis and the presence of IgG anti-insulin Abs at d12 of the response. A scoring system of 0–4 was used to assess insulitis by H&E staining in pancreata sections from unimmunized or insulin-BRT immunized mice (outlined in Methods). NOD mouse pancreata sections served as a positive control for islet infiltration. No insulitis was detected in 60 islets examined in two unimmunized V_H125^{SD} B6 mice or in 82 islets examined in four immunized mice, such that 100% of islets examined received a score of 0. In contrast, 64 islets were scored in two 16–20 wk old female, non-diabetic NOD mice, with 53% islets scoring 0, 14% islets scoring 1, 9% islets scoring 2, 8% islets scoring 3, and 16% islets scoring 4. Endogenous Ig deposition in the islets was assessed by direct immunofluorescence. Ig deposition was not detected in pancreata of either unimmunized or insulin-BRT immunized mice (data not shown). Ig was observed by indirect immunofluorescence, confirming that Abs produced following insulin-BRT immunization are autoreactive. These data indicate that the breach in tolerance driven by insulin-BRT does not elicit a detectable organ-specific autoimmune attack.

Insulin-BRT immunization promotes clonal expansion and restoration of surface IgM for anti-insulin B cells

To assess the fate of anti-insulin B cells undergoing an active breach of tolerance, clonal expansion and proliferation was measured by BrdU incorporation *in vivo* following insulin-BRT immunization. IgM^+ insulin-binding B cells (IgM^{a+} ins^+) in V_H125^{SD} B6 mice immunized with BRT alone (0.33% ± 0.07, n = 7) were not increased compared to unimmunized mice (0.34% ± 0.08, n = 6) (Fig. 5A). In contrast, IgM^+ insulin-binding B cells were expanded in mice immunized with insulin-BRT (2.97% ± 1.28, n = 9) (Fig. 5A). A small population of IgM^- insulin-binding B cells (IgM^{a-} ins^+), that have likely undergone CSR, were detected in V_H125^{SD} B6 mice immunized with insulin-BRT (0.79% ± 0.46, n = 9) but not in unimmunized mice or in mice immunized with BRT alone. BrdU incorporation was used concomitantly to demonstrate that the increase in anti-insulin B cells represented Ag-specific expansion (Fig. 5B). Insulin-binding B cells in V_H125^{SD} B6 mice immunized with BRT alone did not incorporate BrdU and were similar in frequency to that in unimmunized mice. In contrast, both IgM^+ and IgM^- insulin-binding B cell populations in mice immunized with insulin-BRT incorporated BrdU (39.8% ± 7.2 for IgM^+ and 40.5% ± 14.1 for IgM^-, n = 5). These findings correlate with the Ab responses observed in V_H125^{SD} B6 mice following immunization and show that the insulin-BRT conjugate drives clonal expansion and proliferation of anti-insulin B cells *in vivo*.

One hallmark of anergy is reduced surface IgM expression (6, 7, 10). Surface IgM for insulin-binding B cells (ins^+) in unimmunized V_H125^{SD} B6 mice is reduced relative to non-insulin binders (ins^-), expressed as a ratio of mean fluorescence intensity (MFI) of ins^+ to ins^- (0.58 ± 0.12, n = 6). To test whether insulin-BRT immunization promotes restoration of normal surface IgM expression, the MFI of surface IgM was compared for ins^+ and ins^- B cells following immunization (Fig. 5C). Surface IgM for ins^+ B cells was not restored in V_H125^{SD} B6 mice immunized with BRT alone (0.64 ± 0.08, n = 5). In contrast, surface IgM for ins^+ B cells was completely restored following insulin-BRT immunization (1.04 ± 0.09, n = 6). Surface IgM restoration is consistent with reversal of anergy in CSR-competent anti-insulin B cells.

Insulin-specific germinal centers arise in V_H125^{SD} B6 mice

Ig isotype switch in B cells is principally recognized to occur in GC reactions that arise in the follicle following cognate interactions between $CD4^+$ T helper cells and Ag-specific B cells (44–46). Most rapid TI B cell responses are expected to occur in the extrafollicular spaces of the spleen (47), however, it has been demonstrated that some TI B cell responses can promote the unconventional formation of GCs in the absence of T cell help (48, 49). Accordingly, we assessed whether the observed breach in peripheral tolerance for anti-insulin B cells in the insulin-BRT response extends to the formation of GCs. Flow cytometry was used to assess expression of the GC markers, GL7 and Fas, on anti-insulin B cells in V_H125^{SD} B6 mice 5 d following immunization. IgM^+ insulin-binding B cells (IgM^{a+} ins^+) in unimmunized mice established the background for the GC phenotype in the spleen (0.01% $GL7^+$ Fas^+, n = 5), and immunization with BRT alone did not increase this response (0.03% $GL7^+$ Fas^+, n = 7) (Fig. 6A). In striking contrast, IgM^+ insulin-binding B cells in mice immunized with insulin-BRT acquired the GC phenotype (24.4% ± 19.0 $GL7^+$ Fas^+, n = 9) (Fig. 6A). An increased frequency of IgM^- insulin-binding B cells (IgM^{a-} ins^+) acquired the GC phenotype following insulin-BRT immunization (34.2% ± 27.6 $GL7^+$ Fas^+, n = 9), demonstrating that a portion of ins^+ B cells participating in GC reactions have undergone CSR, a finding consistent with production of IgG anti-insulin Abs. Examination of these GC reactions at a later time point in the insulin-BRT response (d12) yielded a sporadic population of ins^+ GC B cells. Three of eight mice examined at d12 had detectable ins^+ GC B cells (5.22 ± 0.08%), while the other five mice did not have a detectable population of the same B cells (0.20 ± 0.13%). Rapid decline in insulin-specific GC B cells and Ab production at d12 following insulin-BRT (data not shown) is consistent with previous work in other models describing the fate of Ag-specific GCs in the absence of cognate T cell help (48). These data support the concept that the insulin-BRT conjugate drives IgG anti-insulin Ab production largely through generation of Ag-specific GCs that are short-lived.

Notably, non-insulin-binding B cells (IgM^{a+} ins^-) in V_H125^{SD} B6 mice did not upregulate GC markers following insulin-BRT immunization (0.39% ± 0.19 $GL7^+$ Fas^+) when compared to unimmunized mice (0.36% ± 0.46 $GL7^+$ Fas^+) (Fig. 6A, top row), suggesting that acquisition of the insulin-specific GC B cell phenotype is limited to cognate anti-insulin B cells and not merely a consequence of global B cell activation from BRT-mediated TLR

stimulation. Flow cytometry staining confirmed that $GL7^+$ Fas^+ GC B cells were IgD^- (Fig. 6B), consistent with induction of a GC B cell phenotype.

To confirm formation of anatomical GCs following insulin-BRT, immunofluorescence staining was performed on spleen sections from both unimmunized and immunized V_H125^{SD} B6 mice. IgM, IgD, and CD3 were used to define follicular architecture, and GCs were identified as IgD^- and $GL7^+$. Whereas some $GL7^+$ IgD^- GCs were observed in unimmunized mice and in mice immunized with BRT alone, they were small by microscopy and non-insulin-specific by flow cytometry (Fig. 6A, C). In contrast, large $GL7^+$ IgD^- GCs were readily detected in spleen sections from mice immunized with insulin-BRT (Fig. 6C). These data show that anti-insulin B cells acquire a GC phenotype and localize to GC structures in the spleen following immunization with insulin-BRT.

Anti-insulin L chains are selected from the pre-immune repertoire to enter germinal center reactions

Anti-insulin B cells are detected in GCs following insulin-BRT immunization (Fig. 6). These GC B cells may reflect expansion of insulin-binding B cells that were present in the pre-immune repertoire (Fig. 3D). Alternatively, the unique environment of GC reactions may select rare anti-insulin B cells that are clonally ignorant or below the level of detection. Accordingly, we investigated selection of anti-insulin Igκ from the pre-immune repertoire by insulin-binding GC B cells. Spleens were harvested from unimmunized V_H125^{SD} B6 mice or from mice immunized with insulin-BRT. Non-GC (IgM^+ $GL7^-$ Fas^-), IgM^+ GC (IgM^+ $GL7^+$ Fas^+), or IgM^- GC (IgM^- $GL7^+$ Fas^+) insulin-binding B cells were purified by flow cytometry sorting as identified in Fig. 5A and Fig. 6A. RNA was purified, and cDNA was used as template for Igκ amplification. The Ig BLAST tool was used to identify Vκ and Jκ gene segment usage (using IMGT nomenclature) as well as any nucleotide mutations (see Methods).

The Vκ125Tg in the previously published anti-insulin 125Tg (H + L chain) mouse model is a Vκ4–74 (25, 50). This L chain is associated with anti-insulin B cells loaded with endogenous rodent insulin detected by mAb123 in V_H125^{SD} B6 mice (Fig. 3D), confirming this Vκ is autoreactive when combined with V_H125. Insulin-binding B cells sorted in unimmunized mice exclusively used Vκ4–74 (Fig. 7A). Vκ4–74 was also the dominant Vκ used by insulin-binding B cells following insulin-BRT immunization, including 11/12 non-GC (Fig. 7B), 8/9 IgM^+ GC, and 5/6 IgM^- GC clones (Fig. 7C–D). Vκ4–74 clones were paired with all Jκ, forming different CDR3 amino acid junctions associated with previously recognized low/moderate (P-L) and high (P-P) affinity for rodent insulin, as deduced from sequences identified in studies of anti-insulin hybridomas (35). The 5’ degenerate primer sequence was removed, and Vκ sequences were deposited into GenBank (http://www.ncbi.nlm.nih.gov/genbank/) with the following accession numbers: unimmunized (KP790058-KP790071), non-GC (KP790072-KP790083), IgM^+ GC (KP790084-KP790092), and IgM^- GC (KP790093-KP790098).

The majority (5/9) of IgM^+ GC anti-insulin B cell clones sorted from V_H125^{SD} B6 mice on d5 following insulin-BRT retained nucleotide sequences in germline Igκ configuration with CDRs identical to those found in unimmunized mice (Fig. 7G). However, an increased

frequency of both IgM^+ and IgM^- GC anti-insulin B cell clones sorted from immunized mice possessed one or more nucleotide mutations relative to non-GC anti-insulin B cells from immunized mice or anti-insulin B cells isolated from unimmunized mice (Fig. 7E–H). Mutations were randomly yet equally distributed in framework regions and CDRs, though no amino acid changes were observed (data not shown). Taken together, these data suggest that anti-insulin B cells enter GCs from the pre-immune repertoire following immunization with the insulin-BRT conjugate, and a proportion of B cells undergo somatic hypermutation in these non-conventional GC reactions.

Discussion

Autoreactive B lymphocytes are recognized to enter the peripheral repertoire of normal individuals, and their presence is considered a liability for developing autoimmune disease. The association of IgG autoAbs with pathological processes suggests that self-reactive B cells are recruited into immune responses. How this occurs is not clear, though a general assumption is that T cell-mediated help is required to reverse tolerance in such B cells. These present studies identify an alternative mechanism by which autoreactive B cells may escape peripheral tolerance without cognate T cell help. We describe the V_H125^{SD} B6 mouse, a new site-directed transgenic model that has a polyclonal B cell repertoire with a detectable population of IgM^+ IgD^+ anti-insulin B cells that have the ability to undergo isotype switch. Anti-insulin B cells in V_H125^{SD} B6 mice are not eliminated but rather rendered clonally anergic in the periphery, unlike other models in which high-affinity Ag-specific B cells are eliminated because they fail to compete in the repertoire for residence in mature compartments (51–53). Tolerance is maintained in CSR-competent anti-insulin B cells following TD immunization, as immunized V_H125^{SD} B6 mice do not produce IgG anti-insulin Abs (Fig. 4A). Immunization of V_H125^{SD} B6 mice with insulin conjugated to a type 1 TI Ag (insulin-BRT), however, provides BCR/TLR co-stimulation that reverses anergy in anti-insulin B cells and promotes proliferation, differentiation into GCs, and IgG autoAb production.

Insulin-BRT was previously used to uncover rare anti-insulin B cells in the repertoires of normal mice independently of T cell help (33). As originally observed, conjugation of insulin and BRT was necessary to drive Ab production (33). As such, immunization of V_H125^{SD} B6 mice with insulin-BRT elicits IgM and IgG2a anti-insulin Abs, whereas neither BRT alone (Fig. 4B) nor BRT physically mixed with insulin (data not shown) elicits Ab production. The kinetics of the insulin-BRT response (3–5 d) and Ab isotypes observed following immunization are in agreement with those seen in response to classic type 1 TI Ags. While insulin-BRT responses have been shown to occur in the absence of T cells (33, 43), they are likely influenced by bystander effects or other non-specific T cell factors, as demonstrated for other TI Ags (54).

Other examples of B cell tolerance reversal independent of T cell help have been described. B cells specific for MHC-I in 3–83 transgenic mice develop normally in the bone marrow but undergo clonal deletion in the periphery when they encounter liver-expressed $H\text{-}2K^b$ (55, 56). However, administration of a bacteriophage containing a 15 amino acid mimotope that is recognized by 3–83 B cells reverses tolerance and drives robust Ig production (55).

Thus, tolerant B cells that are normally deleted in the periphery are actually rescued when self-Ag is presented to the B cell in a TI fashion. Similarly, anergy in anti-insulin B cells is reversed by BCR/TLR co-stimulation in the insulin-BRT response that is relatively TI.

Insulin-specific GCs are found in V_H125^{SD} B6 mice at d5 of the insulin-BRT response (Fig. 6), consistent with previous studies that demonstrated B cells specific for the hapten nitrophenol (NP) can enter GCs without T cell help following immunization with the type 2 TI immunogen NP-Ficoll (48). NP-Ficoll immunization only elicited GCs in QM transgenic mice, which have ~ 60% B cells specific for NP, but not in non-transgenic (WT) littermates. Vinuesa et al. used transfer experiments to confirm that TI GCs only arose when the NP-specific B cell precursor frequency was 1 in 1000 or higher (48). V_H125^{SD} B6 mice possess ~ 0.4% anti-insulin B cells in the periphery (1 in 250), whereas the frequency in WT B6 is closer to 1 in 100,000. As such, we did not observe any detectable insulin-specific GCs in WT mice following insulin-BRT immunization (data not shown), despite IgM and IgG anti-insulin Ab production in the same mice (Fig. 4B). The increased frequency of anti-insulin B cell precursors in V_H125^{SD} B6 mice supports the generation of insulin-specific GCs by d5 and could explain the increased IgM anti-insulin Ab production observed in V_H125^{SD} compared to WT B6 mice. Insulin-specific GCs are found in V_H125^{SD} B6 mice at d12 but at a much lower frequency, as expected for GCs over time in the absence of T cell help. We are currently introducing V_H125^{SD} into NOD mice to determine how these unconventional GC reactions are controlled in an autoimmune strain of mice predisposed to type 1 diabetes.

Igκ genes from the pre-immune repertoire do not undergo negative selection in GCs, as evidenced by exclusive anti-insulin Vκ4–74 usage by BCRs in anti-insulin B cells from unimmunized V_H125^{SD} B6 mice and in IgM+ and IgM- insulin-binding GC B cells from mice following insulin-BRT immunization (Fig. 7). Prior studies show that Vκ4–74 pairs with several Jκ to form autoreactive insulin-binding BCRs when combined with V_H125 (35). Thus, insulin-binding B cells from the pre-immune repertoire, and not obscure clonally ignorant B cells, are selected for GC entry during the insulin-BRT response.

The presence of nucleotide mutations in Vκ4–74 clones indicates somatic hypermutation occurs in these TI GCs. Approximately half of the mutations observed in both IgM+ and IgM- insulin-binding GC clones were found in CDRs, and while amino acid replacements were not observed, the findings suggest that Ag binding could be altered in these atypical GCs. Our data demonstrate that reversal of anergy in anti-insulin B cells provided by BCR/TLR co-stimulation *in vivo* extends to evasion of a tolerance program normally designed to eliminate such autoreactive clones in GCs. While insulin-BRT may not mimic any natural molecule, loss of B cell tolerance via similar pathways may be possible in circumstances where the levels of autoAg and innate stimulus are high, such as on the surface of APCs. This could occur in association with islet inflammation in T1D where APCs are found in close contact with insulin-producing beta cells (57) or following uptake of insulin injected through contaminated skin by epidermal and dermal APCs (58). Recently, TLR-7 signaling was implicated in the development of spontaneous GCs and autoAbs in an SLE model (59), in addition to the previously recognized role of TLR-9 in autoimmune disease (60). Further, BCR/TLR synergy has been shown to induce TI CSR through the non-

canonical NF-κB pathway (61). Thus, there is growing evidence to support a unique role for TLRs in the generation of GCs and production of IgG autoAbs.

We examined the capacity of various TLR mitogens, like ssRNA and CpG DNA, to synergize with insulin *in vitro* to reverse anergy in anti-insulin B cells and found that LPS was the only TLR agonist that enhanced proliferation. BRT contains non-canonical LPS (62–64), thus we expect that the proliferation induced by insulin-BRT *in vivo* (Fig. 5B) occurs in part by TLR-4 stimulation. These data implicate TLR-4 in the reversal of anergy in anti-insulin B cells, though other TLRs are clearly important for tolerance to different autoAgs. The fact that this phenotype occurred at very low stimulating concentrations (Fig. 2E) suggests that signaling thresholds for autoreactive B cells are quite low, and that loss of anergy may arise more quickly and easily than previously thought.

IgG anti-insulin Abs that arise following insulin-BRT immunization were confirmed to be autoreactive by indirect immunofluorescence, as they bound mouse insulin on pancreata sections from both unimmunized and immunized mice. These same autoAbs were not detected endogenously on the tissue using direct immunofluorescence, suggesting that a lack of access of autoAbs to their tissue targets may limit their autoimmune potential. For example, anti-H-2K^{b} Abs generated by phage-mimotope immunization were found on the surfaces of hepatocytes in 3–83 Tg mice (55), reflecting the ubiquitous surface expression of MHC-I in the target organ. Access to insulin epitopes may be more restricted in the islets. Experiments in V_H125^{SD} NOD mice will determine if reversal of anergy in anti-insulin B cells driven by BCR/TLR co-stimulation accelerates immunopathology.

Type 1 diabetes in mice and humans is a multigenic autoimmune disorder in which detection of IgG insulin autoAbs indicates that loss of tolerance in anti-insulin B cells is a critical event in disease pathogenesis. We show evidence that this breach in the B cell compartment surprisingly does not depend on T cell help. Common environmental triggers resulting from infection and inflammation that are prevalent in children could combine with endogenous insulin to break anti-insulin B cell tolerance. BCR/TLR co-stimulation of autoreactive B lymphocytes could represent an early, under-appreciated event in the induction of autoimmunity.

Supplementary Material

Refer to Web version on PubMed Central for supplementary material.

Acknowledgements

We thank Dr. Klaus Rajewsky for providing the pIV$_H$L2neoR targeting vector, and we thank Dr. Richard Breyer for EIIA-Cre B6 mice. We thank the Vanderbilt Technologies for Advanced Genomics Sequencing Core, the Transgenic Mouse/Embryonic Stem Cell Shared Resource, the Vanderbilt Flow Cytometry Shared Resource, and the Translational Pathology Shared Resource. We thank the Division of Animal Care for their assistance in the maintenance of the mice. We also graciously thank Dr. John Williams, Dr. Daniel Moore, and Dr. Damian Maseda for critical review of the manuscript.

This work was supported by National Institutes of Health (NIH) T32 AR059039, AI051448, Juvenile Diabetes Research Foundation 1-2005-167, 3-2013-121, and the Vanderbilt Diabetes Research and Training Center (DK20593). The Vanderbilt Flow Cytometry Shared Resource Core is supported by the Vanderbilt Ingram Cancer Center (P30 CA068485) and the Vanderbilt Digestive Disease Research Center (DK058404). The Vanderbilt

Transgenic/Embryonic Stem Cell Shared Resource Core is supported by The Cancer Center Support NIH Grant (CA068485), the Vanderbilt Diabetes Research and Training Center (DK20593), the Vanderbilt Brain Institute, and the Center for Stem Cell Biology. The Vanderbilt Technologies for Advanced Genomics Sequencing Facility is supported by the Vanderbilt Ingram Cancer Center (P30 CA68485), the Vanderbilt Vision Center (P30 EY08126), and the NIH/National Center for Research Resources (G20 RR030956). The Vanderbilt Translational Pathology Shared Resource Core is supported by the Mouse Metabolic and Phenotyping Center (DK059637).

Abbreviations Used

B6	C57BL/6
BRT	*Brucella abortus* ring test antigen
CSR	Class switch recombination
FO	Follicular
GC	Germinal center
HEL	Hen egg lysozyme
MZ	Marginal zone
T1	Transitional 1
TD	T cell-dependent
TI	T cell-independent

References

1. Pelanda R, Torres RM. Central B-cell tolerance: where selection begins. Cold Spring Harbor perspectives in biology. 2012; 4:a007146. [PubMed: 22378602]
2. Casellas R, Shih TA, Kleinewietfeld M, Rakonjac J, Nemazee D, Rajewsky K, Nussenzweig MC. Contribution of receptor editing to the antibody repertoire. Science. 2001; 291:1541–1544. [PubMed: 11222858]
3. Radic MZ, Erikson J, Litwin S, Weigert M. B lymphocytes may escape tolerance by revising their antigen receptors. The Journal of experimental medicine. 1993; 177:1165–1173. [PubMed: 8459210]
4. Nemazee D, Buerki K. Clonal deletion of autoreactive B lymphocytes in bone marrow chimeras. Proceedings of the National Academy of Sciences of the United States of America. 1989; 86:8039–8043. [PubMed: 2682636]
5. Chen C, Nagy Z, Prak EL, Weigert M. Immunoglobulin heavy chain gene replacement: a mechanism of receptor editing. Immunity. 1995; 3:747–755. [PubMed: 8777720]
6. Cambier JC, Gauld SB, Merrell KT, Vilen BJ. B-cell anergy: from transgenic models to naturally occurring anergic B cells? Nature reviews. Immunology. 2007; 7:633–643.
7. Yarkoni Y, Getahun A, Cambier JC. Molecular underpinning of B-cell anergy. Immunological reviews. 2010; 237:249–263. [PubMed: 20727040]
8. Sakaguchi S, Wing K, Onishi Y, Prieto-Martin P, Yamaguchi T. Regulatory T cells: how do they suppress immune responses? International immunology. 2009; 21:1105–1111. [PubMed: 19737784]
9. Kim J, Lahl K, Hori S, Loddenkemper C, Chaudhry A, deRoos P, Rudensky A, Sparwasser T. Cutting edge: depletion of Foxp3+ cells leads to induction of autoimmunity by specific ablation of regulatory T cells in genetically targeted mice. Journal of immunology. 2009; 183:7631–7634.
10. Goodnow CC, Crosbie J, Adelstein S, Lavoie TB, Smith-Gill SJ, Brink RA, Pritchard-Briscoe H, Wotherspoon JS, Loblay RH, Raphael K, et al. Altered immunoglobulin expression and functional silencing of self-reactive B lymphocytes in transgenic mice. Nature. 1988; 334:676–682. [PubMed: 3261841]

11. Goodnow CC, Crosbie J, Jorgensen H, Brink RA, Basten A. Induction of self-tolerance in mature peripheral B lymphocytes. Nature. 1989; 342:385–391. [PubMed: 2586609]
12. Getahun A, O'Neill SK, Cambier JC. Establishing anergy as a bona fide in vivo mechanism of B cell tolerance. Journal of immunology. 2009; 183:5439–5441.
13. Merrell KT, Benschop RJ, Gauld SB, Aviszus K, Decote-Ricardo D, Wysocki LJ, Cambier JC. Identification of anergic B cells within a wild-type repertoire. Immunity. 2006; 25:953–962. [PubMed: 17174121]
14. Hikida M, Kurosaki T. Regulation of phospholipase C-gamma2 networks in B lymphocytes. Advances in immunology. 2005; 88:73–96. [PubMed: 16227088]
15. Fruman DA, Bismuth G. Fine tuning the immune response with PI3K. Immunological reviews. 2009; 228:253–272. [PubMed: 19290933]
16. Menard L, Saadoun D, Isnardi I, Ng YS, Meyers G, Massad C, Price C, Abraham C, Motaghedi R, Buckner JH, Gregersen PK, Meffre E. The PTPN22 allele encoding an R620W variant interferes with the removal of developing autoreactive B cells in humans. The Journal of clinical investigation. 2011; 121:3635–3644. [PubMed: 21804190]
17. Avalos AM, Busconi L, Marshak-Rothstein A. Regulation of autoreactive B cell responses to endogenous TLR ligands. Autoimmunity. 2010; 43:76–83. [PubMed: 20014959]
18. Avalos AM, Uccellini MB, Lenert P, Viglianti GA, Marshak-Rothstein A. FcgammaRIIB regulation of BCR/TLR-dependent autoreactive B-cell responses. European journal of immunology. 2010; 40:2692–2698. [PubMed: 20809520]
19. Maglione PJ, Simchoni N, Black S, Radigan L, Overbey JR, Bagiella E, Bussel JB, Bossuyt X, Casanova JL, Meyts I, Cerutti A, Picard C, Cunningham-Rundles C. IRAK-4 and MyD88 deficiencies impair IgM responses against T-independent bacterial antigens. Blood. 2014; 124:3561–3571. [PubMed: 25320238]
20. Dye JR, Palvanov A, Guo B, Rothstein TL. B cell receptor cross-talk: exposure to lipopolysaccharide induces an alternate pathway for B cell receptor-induced ERK phosphorylation and NF-kappa B activation. Journal of immunology. 2007; 179:229–235.
21. Kendall PL, Yu G, Woodward EJ, Thomas JW. Tertiary lymphoid structures in the pancreas promote selection of B lymphocytes in autoimmune diabetes. Journal of immunology. 2007; 178:5643–5651.
22. Kendall PL, Case JB, Sullivan AM, Holderness JS, Wells KS, Liu E, Thomas JW. Tolerant anti-insulin B cells are effective APCs. Journal of immunology. 2013; 190:2519–2526.
23. Yalow RS, Berson SA. Immunoassay of endogenous plasma insulin in man. The Journal of clinical investigation. 1960; 39:1157–1175. [PubMed: 13846364]
24. Schroer JA, Inman JK, Thomas JW, Rosenthal AS. H-2-linked Ir gene control of antibody responses to insulin. I. Anti-insulin plaque-forming cell primary responses. Journal of immunology. 1979; 123:670–675.
25. Rojas M, Hulbert C, Thomas JW. Anergy and not clonal ignorance determines the fate of B cells that recognize a physiological autoantigen. Journal of immunology. 2001; 166:3194–3200.
26. Acevedo-Suarez CA, Hulbert C, Woodward EJ, Thomas JW. Uncoupling of anergy from developmental arrest in anti-insulin B cells supports the development of autoimmune diabetes. Journal of immunology. 2005; 174:827–833.
27. Koczwara K, Schenker M, Schmid S, Kredel K, Ziegler AG, Bonifacio E. Characterization of antibody responses to endogenous and exogenous antigen in the nonobese diabetic mouse. Clinical immunology. 2003; 106:155–162. [PubMed: 12672406]
28. Boes M, Schmidt T, Linkemann K, Beaudette BC, Marshak-Rothstein A, Chen J. Accelerated development of IgG autoantibodies and autoimmune disease in the absence of secreted IgM. Proceedings of the National Academy of Sciences of the United States of America. 2000; 97:1184–1189. [PubMed: 10655505]
29. Hoppu S, Ronkainen MS, Kimpimaki T, Simell S, Korhonen S, Ilonen J, Simell O, Knip M. Insulin autoantibody isotypes during the prediabetic process in young children with increased genetic risk of type 1 diabetes. Pediatric research. 2004; 55:236–242. [PubMed: 14605243]
30. Hahn BH. Antibodies to DNA. The New England journal of medicine. 1998; 338:1359–1368. [PubMed: 9571257]

31. Zhang L, Nakayama M, Eisenbarth GS. Insulin as an autoantigen in NOD/human diabetes. Current opinion in immunology. 2008; 20:111–118. [PubMed: 18178393]
32. Nakayama M. Insulin as a key autoantigen in the development of type 1 diabetes. Diabetes/metabolism research and reviews. 2011; 27:773–777. [PubMed: 22069258]
33. Thomas JW, Bucy RP, Kapp JA. T cell-independent responses to an Ir gene-controlled antigen. I. Characteristics of the immune response to insulin complexed to Brucella abortus. Journal of immunology. 1982; 129:6–10.
34. Pewzner-Jung Y, Friedmann D, Sonoda E, Jung S, Rajewsky K, Eilat D. B cell deletion, anergy, and receptor editing in "knock in" mice targeted with a germline-encoded or somatically mutated anti-DNA heavy chain. Journal of immunology. 1998; 161:4634–4645.
35. Henry-Bonami RA, Williams JM, Rachakonda AB, Karamali M, Kendall PL, Thomas JW. B lymphocyte "original sin" in the bone marrow enhances islet autoreactivity in type 1 diabetes-prone nonobese diabetic mice. Journal of immunology. 2013; 190:5992–6003.
36. Thomas JW, Virta VJ, Nell LJ. Idiotypic determinants on human anti-insulin antibodies are cyclically expressed. Journal of immunology. 1986; 137:1610–1615.
37. Woodward EJ, Thomas JW. Multiple germline kappa light chains generate anti-insulin B cells in nonobese diabetic mice. Journal of immunology. 2005; 175:1073–1079.
38. Henry RA, Kendall PL, Woodward EJ, Hulbert C, Thomas JW. Vkappa polymorphisms in NOD mice are spread throughout the entire immunoglobulin kappa locus and are shared by other autoimmune strains. Immunogenetics. 2010; 62:507–520. [PubMed: 20556377]
39. Phan TG, Amesbury M, Gardam S, Crosbie J, Hasbold J, Hodgkin PD, Basten A, Brink R. B cell receptor-independent stimuli trigger immunoglobulin (Ig) class switch recombination and production of IgG autoantibodies by anergic self-reactive B cells. The Journal of experimental medicine. 2003; 197:845–860. [PubMed: 12668643]
40. Liu Z, Davidson A. BAFF and selection of autoreactive B cells. Trends in immunology. 2011; 32:388–394. [PubMed: 21752714]
41. Enzler T, Bonizzi G, Silverman GJ, Otero DC, Widhopf GF, Anzelon-Mills A, Rickert RC, Karin M. Alternative and classical NF-kappa B signaling retain autoreactive B cells in the splenic marginal zone and result in lupus-like disease. Immunity. 2006; 25:403–415. [PubMed: 16973390]
42. Gavin AL, Hoebe K, Duong B, Ota T, Martin C, Beutler B, Nemazee D. Adjuvant-enhanced antibody responses in the absence of toll-like receptor signaling. Science. 2006; 314:1936–1938. [PubMed: 17185603]
43. Mond JJ, Scher I, Mosier DE, Baese M, Paul WE. T-independent responses in B cell-defective CBA/N mice to Brucella abortus and to trinitrophenyl (TNP) conjugates of Brucella abortus. European journal of immunology. 1978; 8:459–463. [PubMed: 99320]
44. Gitlin AD, Shulman Z, Nussenzweig MC. Clonal selection in the germinal centre by regulated proliferation and hypermutation. Nature. 2014; 509:637–640. [PubMed: 24805232]
45. Baumjohann D, Preite S, Reboldi A, Ronchi F, Ansel KM, Lanzavecchia A, Sallusto F. Persistent antigen and germinal center B cells sustain T follicular helper cell responses and phenotype. Immunity. 2013; 38:596–605. [PubMed: 23499493]
46. Qi H, Cannons JL, Klauschen F, Schwartzberg PL, Germain RN. SAP-controlled T-B cell interactions underlie germinal centre formation. Nature. 2008; 455:764–769. [PubMed: 18843362]
47. Fagarasan S, Honjo T. T-Independent immune response: new aspects of B cell biology. Science. 2000; 290:89–92. [PubMed: 11021805]
48. de Vinuesa CG, Cook MC, Ball J, Drew M, Sunners Y, Cascalho M, Wabl M, Klaus GG, MacLennan IC. Germinal centers without T cells. The Journal of experimental medicine. 2000; 191:485–494. [PubMed: 10662794]
49. Wang D, Wells SM, Stall AM, Kabat EA. Reaction of germinal centers in the T-cell-independent response to the bacterial polysaccharide alpha(1-->6)dextran. Proceedings of the National Academy of Sciences of the United States of America. 1994; 91:2502–2506. [PubMed: 7511812]
50. Ewulonu UK, Nell LJ, Thomas JW. VH and VL gene usage by murine IgG antibodies that bind autologous insulin. Journal of immunology. 1990; 144:3091–3098.

51. Hartley SB, Crosbie J, Brink R, Kantor AB, Basten A, Goodnow CC. Elimination from peripheral lymphoid tissues of self-reactive B lymphocytes recognizing membrane-bound antigens. Nature. 1991; 353:765–769. [PubMed: 1944535]
52. Wang H, Shlomchik MJ. High affinity rheumatoid factor transgenic B cells are eliminated in normal mice. Journal of immunology. 1997; 159:1125–1134.
53. Cyster JG, Hartley SB, Goodnow CC. Competition for follicular niches excludes self-reactive cells from the recirculating B-cell repertoire. Nature. 1994; 371:389–395. [PubMed: 7522305]
54. Endres RO, Kushnir E, Kappler JW, Marrack P, Kinsky SC. A requirement for nonspecific T cell factors in antibody responses to "T cell independent" antigens. Journal of immunology. 1983; 130:781–784.
55. Kouskoff V, Lacaud G, Nemazee D. T cell-independent rescue of B lymphocytes from peripheral immune tolerance. Science. 2000; 287:2501–2503. [PubMed: 10741972]
56. Caucheteux SM, Vernochet C, Wantyghem J, Gendron MC, Kanellopoulos-Langevin C. Tolerance induction to self-MHC antigens in fetal and neonatal mouse B cells. International immunology. 2008; 20:11–20. [PubMed: 18032373]
57. Mohan JF, Levisetti MG, Calderon B, Herzog JW, Petzold SJ, Unanue ER. Unique autoreactive T cells recognize insulin peptides generated within the islets of Langerhans in autoimmune diabetes. Nature immunology. 2010; 11:350–354. [PubMed: 20190756]
58. Levin C, Perrin H, Combadiere B. Tailored immunity by skin antigen-presenting cells. Human vaccines & immunotherapeutics. 2014:e34299.
59. Soni C, Wong EB, Domeier PP, Khan TN, Satoh T, Akira S, Rahman ZS. B Cell-Intrinsic TLR7 Signaling Is Essential for the Development of Spontaneous Germinal Centers. Journal of immunology. 2014; 193:4400–4414.
60. Christensen SR, Kashgarian M, Alexopoulou L, Flavell RA, Akira S, Shlomchik MJ. Toll-like receptor 9 controls anti-DNA autoantibody production in murine lupus. The Journal of experimental medicine. 2005; 202:321–331. [PubMed: 16027240]
61. Pone EJ, Zhang J, Mai T, White CA, Li G, Sakakura JK, Patel PJ, Al-Qahtani A, Zan H, Xu Z, Casali P. BCR-signalling synergizes with TLR-signalling for induction of AID and immunoglobulin class-switching through the non-canonical NF-kappaB pathway. Nature communications. 2012; 3:767.
62. Forestier C, Moreno E, Meresse S, Phalipon A, Olive D, Sansonetti P, Gorvel JP. Interaction of Brucella abortus lipopolysaccharide with major histocompatibility complex class II molecules in B lymphocytes. Infection and immunity. 1999; 67:4048–4054. [PubMed: 10417173]
63. Betts M, Beining P, Brunswick M, Inman J, Angus RD, Hoffman T, Golding B. Lipopolysaccharide from Brucella abortus behaves as a T-cell-independent type 1 carrier in murine antigen-specific antibody responses. Infection and immunity. 1993; 61:1722–1729. [PubMed: 8478060]
64. Weiss DS, Takeda K, Akira S, Zychlinsky A, Moreno E. MyD88, but not toll-like receptors 4 and 2, is required for efficient clearance of Brucella abortus. Infection and immunity. 2005; 73:5137–5143. [PubMed: 16041030]

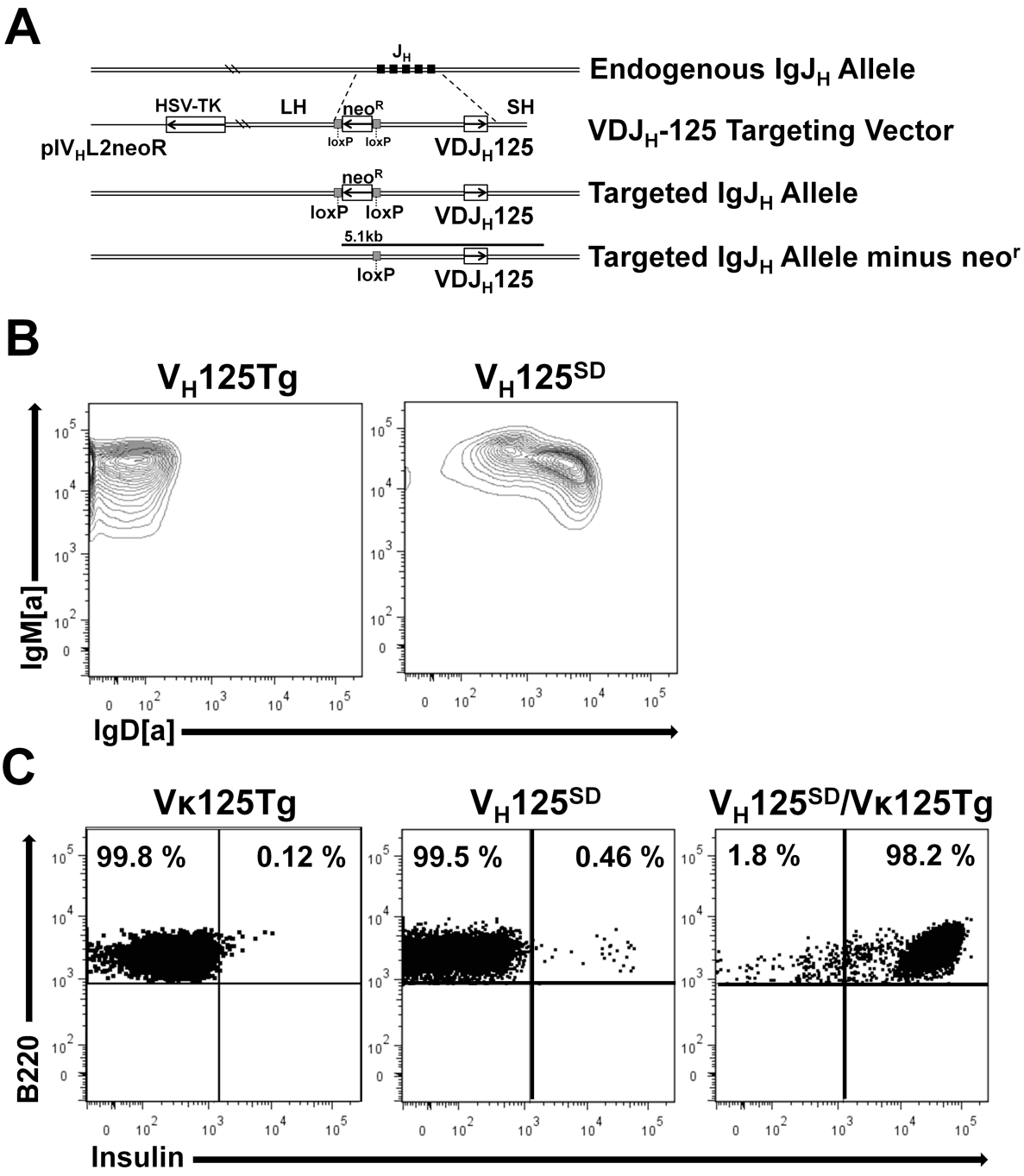

Figure 1. A site-directed BCR transgenic mouse model generates class switch-competent anti-insulin B lymphocytes

(A) Strategy for targeting anti-insulin VDJ_H-125 to the Ig H chain locus (site-directed V_H125^{SD}). **(B)** Flow cytometry was used to assess IgM and IgD expression on B cells ($B220^+$ live lymphocytes) from spleens of V_H125^{SD} B6 mice (right) and conventional IgM-restricted, non-site-directed V_H125Tg B cells (left). **(C)** Insulin-binding B cells identified by flow cytometry in Vκ125Tg B6 mice (left), site-directed V_H125^{SD} B6 mice (middle), and in mice that harbor both V_H125^{SD} and Vκ125Tg (right).

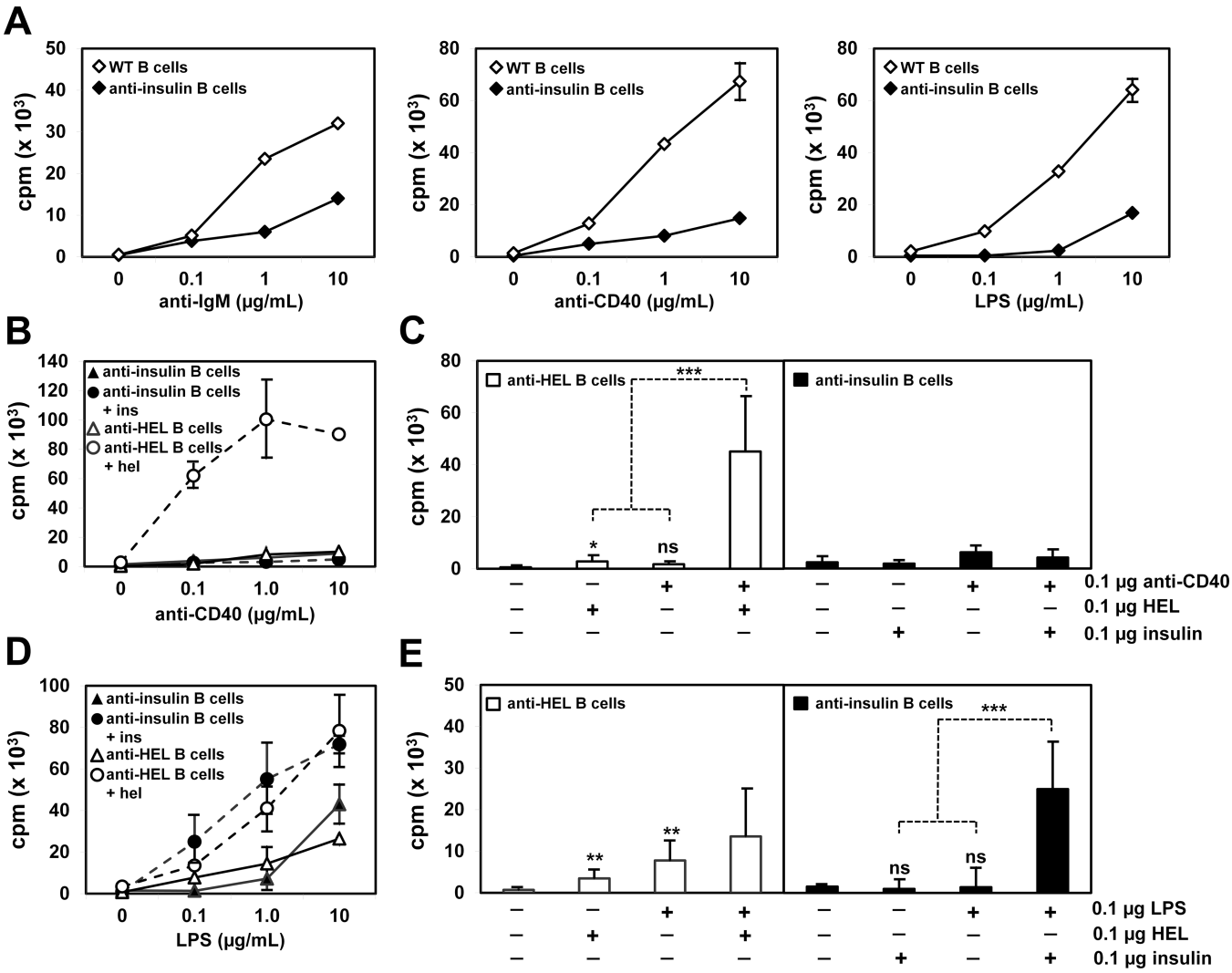

Figure 2. Anergy in anti-insulin B cells is reversed by TLR-4 but not CD40 co-stimulation in vitro

B cells were CD43 MACS purified from either V_H125^{SD}/Vκ125Tg, or control MD4 anti-HEL Tg or wild-type (WT) B6 mice. **(A)** B cells from WT and V_H125^{SD}/Vκ125Tg mice were cultured for 72 h to a dose response of anti-IgM, anti-CD40, or LPS. B cells from V_H125^{SD}/Vκ125Tg and MD4 anti-HEL Tg mice were cultured to a dose response of anti-CD40 **(B)** or LPS **(D)** with or without 0.1 μg/mL insulin or HEL Ag. The proliferative response at the combined suboptimal dose of 0.1 μg/mL is shown for both anti-CD40 **(C)** and LPS **(E)** stimuli plus Ag. B cells received a 1 μCi pulse of tritiated thymidine 48h into culture before harvest at 72h. For anti-CD40 studies, n = 6 for both V_H125^{SD}/Vκ125Tg and MD4 anti-HEL Tg mice. For LPS studies, n = 9 for V_H125^{SD}/Vκ125Tg and n = 8 for MD4 anti-HEL Tg mice. Data represent at least three independent experiments. * $p < 0.05$, ** $p < 0.01$, *** $p < 0.001$, two-tailed t test. ns, not significant.

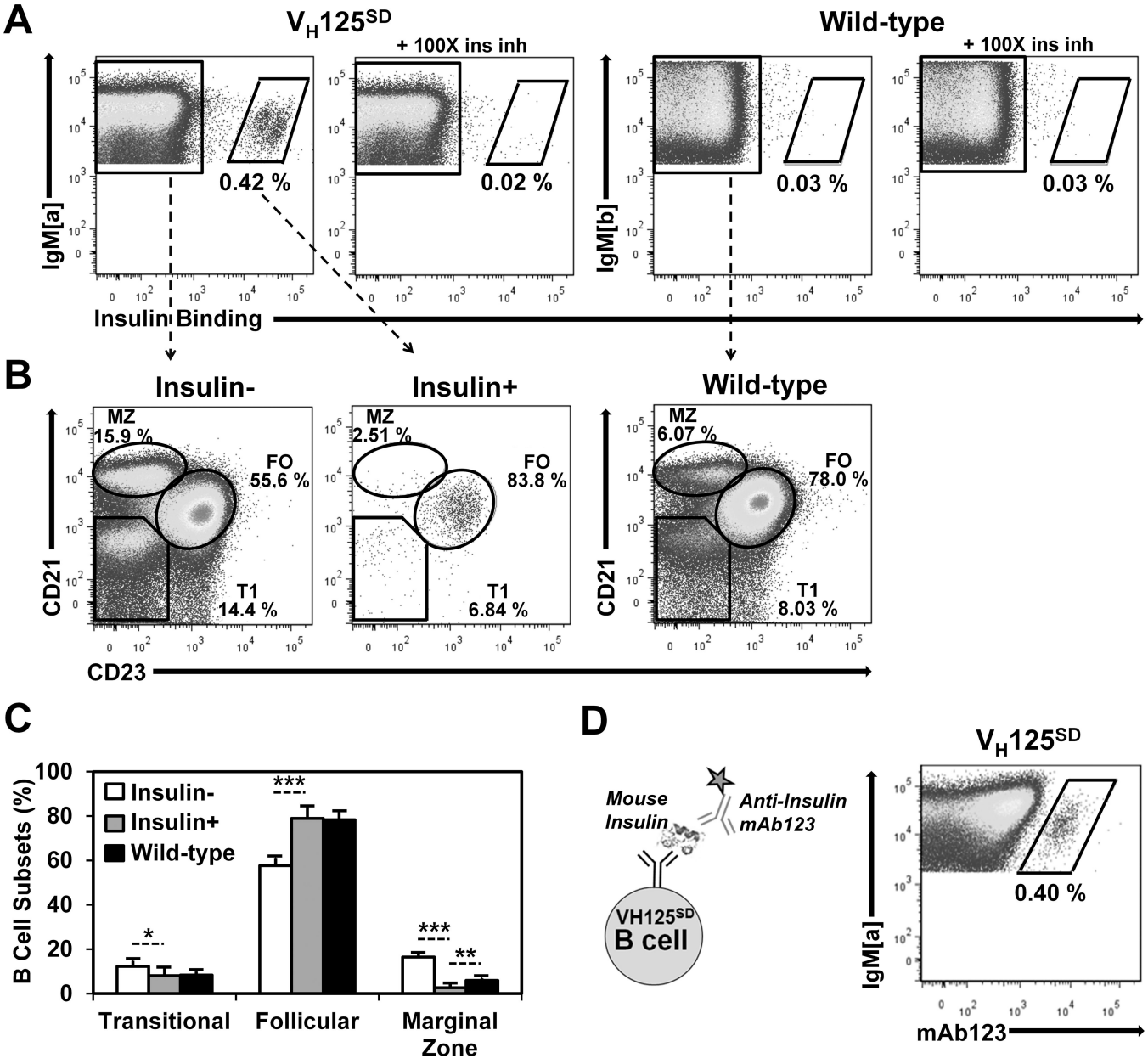

Figure 3. Anti-insulin B cells from V_H125^{SD} B6 mice undergo peripheral maturation

(A) Splenocytes were gated on $B220^+$ IgM^+ live lymphocytes. Splenocytes were harvested from V_H125^{SD} (left) or WT (right) B6 mice and were incubated with 17 nM biotinylated human insulin with or without 100× free insulin to detect insulin-specific B cells using flow cytometry. Anti-IgM^a detects transgenic B cells; anti-IgM^b detects WT B cells **(B)** CD21 and CD23 expression were used to define Transitional 1 (T1), Follicular (FO), or Marginal Zone (MZ) B cell subset distribution of insulin (left), $insulin^+$ (middle), or WT (right) B cells, quantified in **(C)** as subset percentage of IgM^+ B cells. **(D)** Biotinylated anti-insulin mAb123, depicted in the schematic (left), was used to detect V_H125^{SD} B cells that bind endogenous rodent insulin (right). * $p < 0.05$, ** $p < 0.01$, *** $p < 0.001$, two-tailed t test.

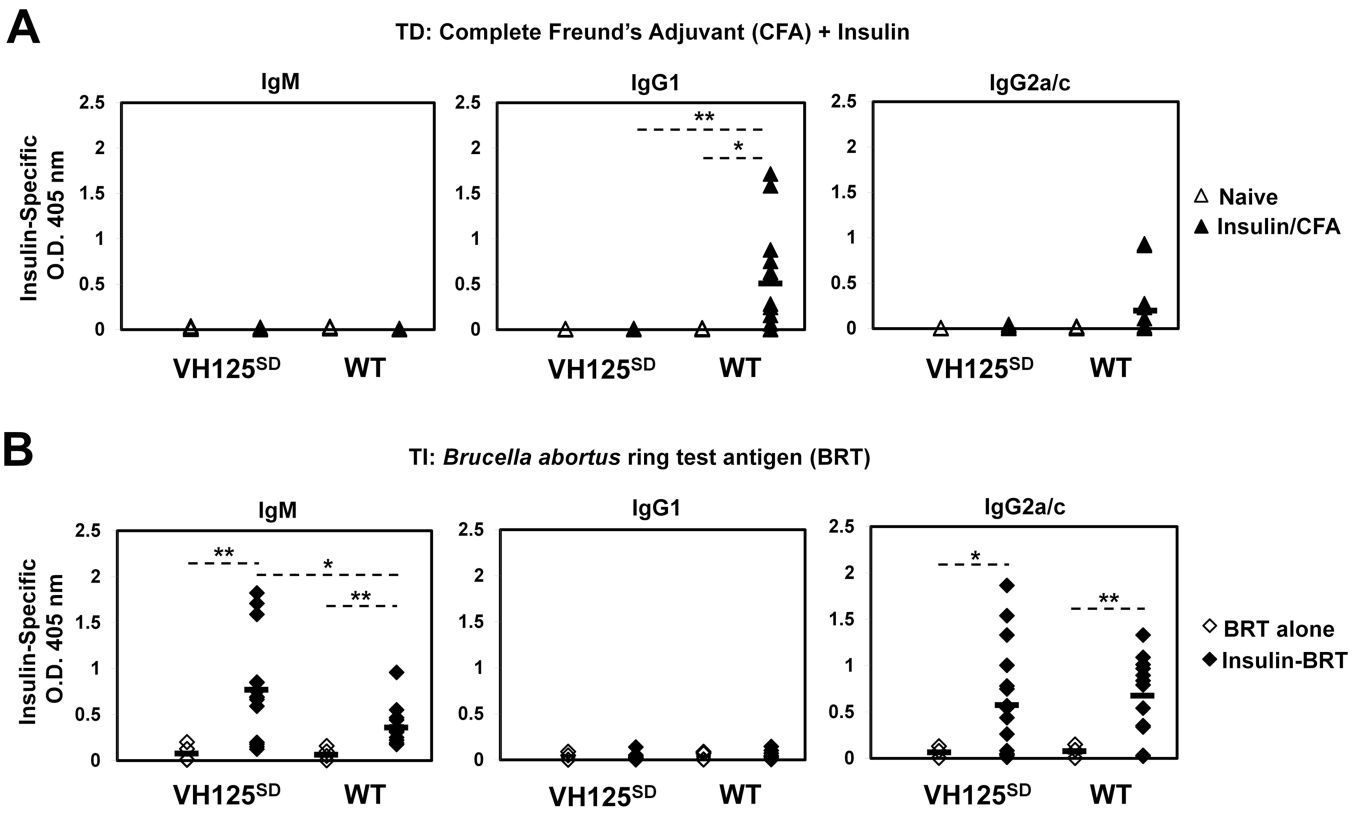

Figure 4. IgM and IgG anti-insulin antibodies are produced in V_H125^{SD} B6 mice following TI but not TD immunization

V_H125^{SD} and WT B6 mice were immunized with either bovine insulin in 1X PBS emulsified in CFA (insulin/CFA) s.c. base of the tail, or *Brucella abortus* ring test Ag (BRT) alone, or human insulin conjugated to BRT (insulin-BRT) i.p. in 1X PBS. **(A)** Insulin-specific IgM^a, $IgG1^a$, and $IgG2a^a$ (V_H125^{SD}) or IgM^b, $IgG1^b$, and $IgG2c^b$ (WT) in sera was measured by ELISA before (open) and 2–3 wks following TD immunization with insulin/CFA (closed). **(B)** Insulin-specific IgM, IgG1, and IgG2a/c in sera was measured by ELISA 5–7 d following immunization with BRT alone (open) or insulin-BRT (closed). For insulin/CFA, n = 12 for both V_H125^{SD} and WT. For insulin-BRT, n = 12 V_H125^{SD} and n = 10 WT. For BRT alone, n = 6 mice per group. Data represent at least three independent experiments. * $p < 0.05$, ** $p < 0.01$, *** $p < 0.001$, two-tailed t test.

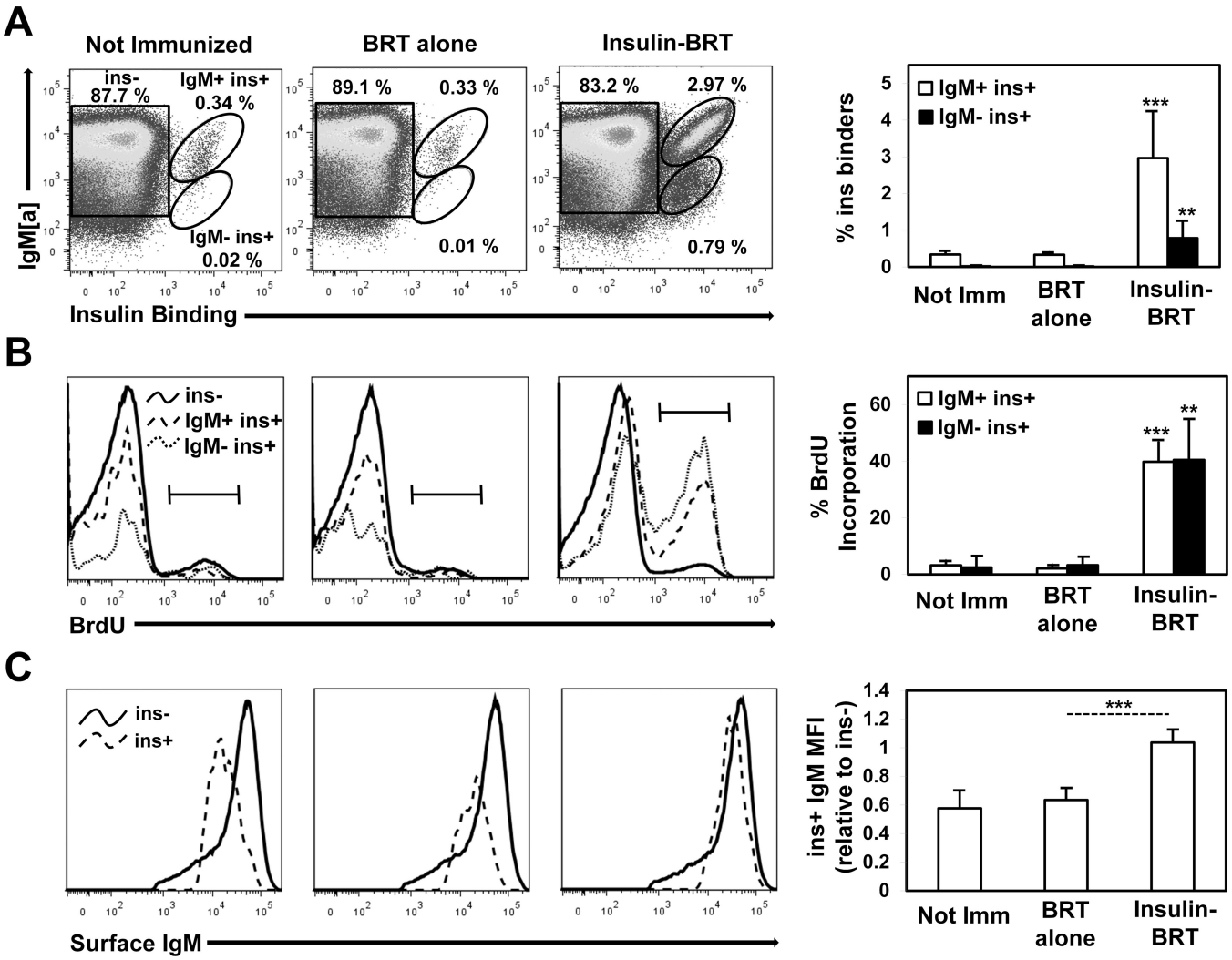

Figure 5. Insulin-BRT immunization promotes clonal expansion and restoration of surface IgM for anti-insulin B cells

V_H125^{SD} B6 mice were not immunized (n = 6) or immunized with either BRT alone (n = 7) or insulin-BRT (n = 9) i.p. in 1X PBS. **(A)** Insulin-binding B cells ($B220^+$ live lymphocytes) in the spleen were quantified 5 d following immunization by flow cytometry. Representative plots (left) and averages (right) are shown. **(B)** Mice were injected twice with BrdU i.p. 48h and 24h before sacrifice, and intracellular BrdU incorporation was measured in non-insulin binders (ins, solid black line), IgM^+ insulin binders (IgM^+ ins^+, dashed line), and IgM insulin binders (IgM ins^+, fine dashed line). Representative histograms (left) and averages (right) are shown. **(C)** The mean fluorescence intensity (MFI) of surface IgM for ins and ins^+ B cells is shown in representative histograms (left) and is also expressed as a ratio of ins^+/ins IgM MFI average ± SD (right). Data represent at least three independent experiments. Unless otherwise indicated, statistical comparisons are to unimmunized mice. * $p < 0.05$, ** $p < 0.01$, *** $p < 0.001$, two-tailed t test.

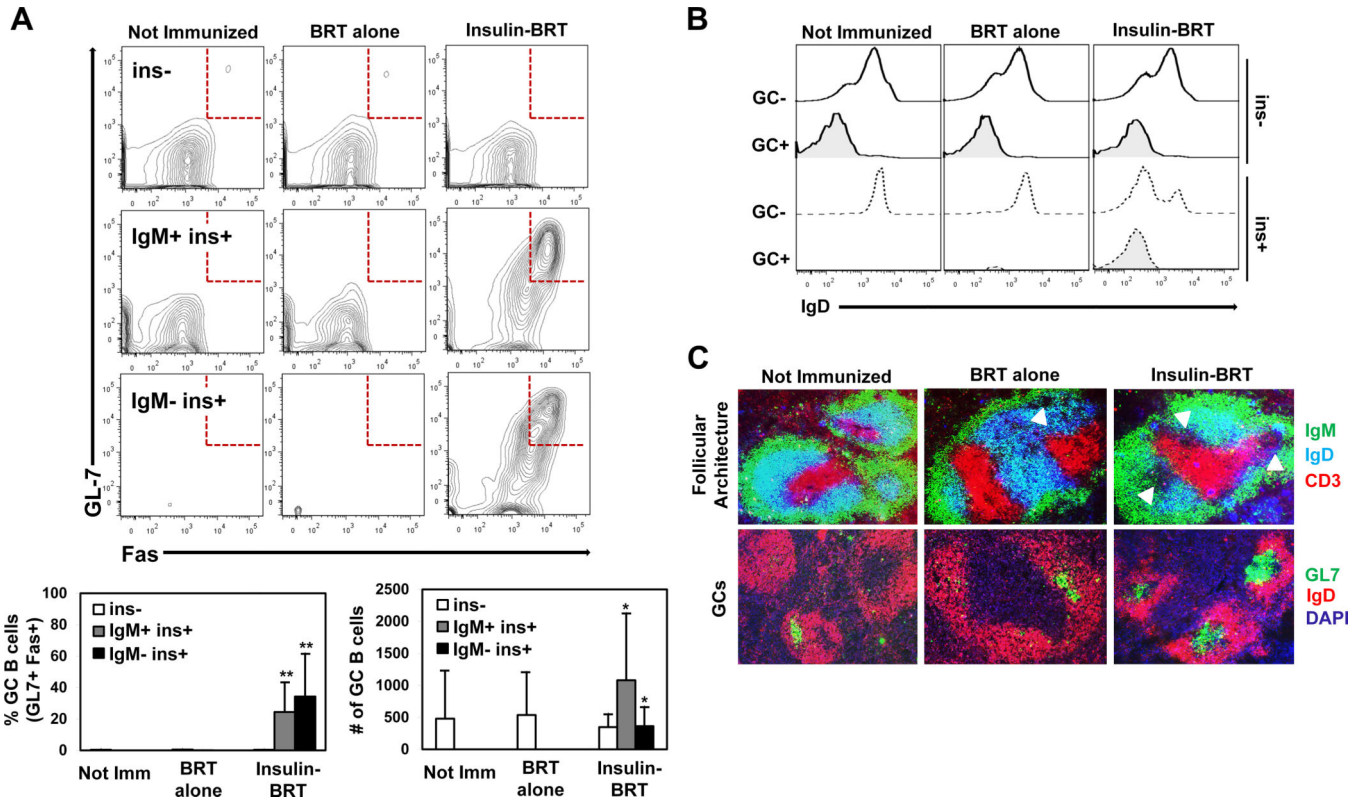

Figure 6. Insulin-specific germinal centers arise in V_H125^{SD} B6 mice

V_H125^{SD} B6 mice were immunized with either BRT alone or insulin-BRT i.p. in 1X PBS. **(A)** Flow cytometry was used to assess GC B cell phenotype by GL7 and Fas expression on B cells ($B220^+$ live lymphocytes) separated into non-insulin binders (ins, white), IgM^+ insulin binders (IgM^+ ins^+, gray), and IgM insulin binders (IgM ins^+, black). Representative plots (top) and GC B cell subset percent and cell number averages (bottom) are shown. **(B)** IgD expression was measured for ins (solid black line) and ins^+ B cells (dashed line) following immunization, and representative histograms are shown. **(C)** Immunofluorescence microscopy detected follicular architecture (top, IgD CD3, GCs indicated by arrows) and GC structures (bottom, $GL7^+$ IgD) in spleens from V_H125^{SD} B6 mice (n = 4). Follicles counted: n = 21 not immunized, n = 12 BRT alone, and n = 17 insulin-BRT. Data represent at least three independent experiments. Unless otherwise indicated, statistical comparisons are to unimmunized mice. * $p < 0.05$, ** $p < 0.01$, *** $p < 0.001$, two-tailed t test.

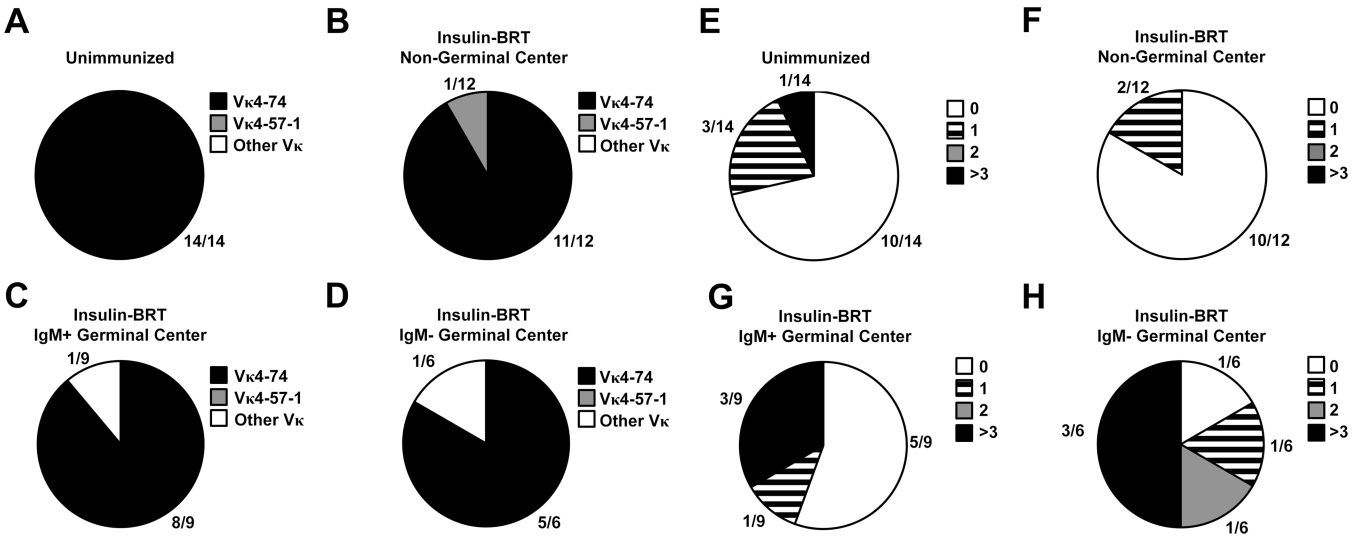

Figure 7. Anti-insulin L chains are selected from the pre-immune repertoire to enter germinal center reactions

Spleens were harvested from unimmunized V_H125^{SD} B6 mice, or from mice 4 d following immunization with insulin-BRT. Flow cytometry sorting was using to purify insulin-binding B cells ($B220^+$ live lymphocytes), that were further gated in immunized mice as IgM^+ non-GC (GL7 Fas), IgM^+ GC ($GL7^+$ Fas^+), or IgM GC populations. Isolated RNA was transcribed to cDNA, and Igκ genes were amplified by PCR. Sequences were analyzed using the Ig BLAST database (see Methods). **(A-D)** The number of clones identified by the indicated Vκ is divided by the total number of clones analyzed for each immunization group. Vκ4–74 (black), Vκ4–57–1 (gray), all other Vκ (white). **(E-H)** Igκ clone sequences were compared to germline sequences, excluding the 5' region that correlated with degenerate primers used for amplification. The number of sequences that possess the indicated number of nucleotide changes, 0 (white), 1 (striped), 2 (gray), or > 3 (black), is shown for each immunization group.